Proceedings of the IEEE 20th Conference on Electrical Performance of Electronic Packaging and Systems, EPEPS 2011, San Jose, pp. 119-122, Oct. 23-26, 2011

An Analytical Resistive Loss Model for Multiconductor Transmission Lines and the Proof of its Passivity

Frédéric Broydé and Evelyne Clavelier
Tekcem
12, chemin des Hauts de Clairefontaine, 78580 Maule, France
tel: +33 1 34 75 13 65 e-mail: {fredbroyde,eclavelier}@tekcem.com

***Abstract* — A new model for resistive losses can be used within the multiconductor transmission line model of a multiconductor interconnection. It provides accurate results at low and high frequencies. We prove that this model is passive.**

***Keywords* — Multiconductor transmission lines, resistive loss model, signal integrity analysis.**

I. Introduction

This paper is about a model for the resistive losses in a multiconductor interconnection. This model was created for investigating innovative on-chip or chip-to-chip signaling schemes. In this context, one wishes to handily vary the length of the interconnection, so that it is advantageous to use a multiconductor transmission line (MTL) model for one or more segments of the interconnection. Usually this will be a uniform MTL model, in which the length of a segment is easily changed using a single simulation parameter, as opposed to a macromodel which is synthesized for a fixed length. Thus, the loss model must provide a per-unit-length (p.u.l.) impedance matrix.

In this paper, we do not try to take into account characteristics which might occur but are not necessarily present, such as plating and/or roughness of the conductors, anisotropy of a composite substrate, etc. We are also not interested in discontinuities such as vias, crossing conductors, packaging parasitics, etc. We propose a closed-form model for the p.u.l. internal impedance matrix of a uniform multiconductor interconnection complying with these assumptions and having n transmission conductors (TCs) and a reference or ground conductor (GC). The cross-section of such a $(n+1)$-conductor interconnection is shown in Fig. 1, in the special case of a simple multiconductor microstrip structure.

In a previous paper [1], the authors have presented a simple method for computing a high-frequency (h.f.) current distribution in the cross-section of the interconnection, which takes into account the normal skin effect, the crowding of currents at the edges of each conductor (edge effect), and the interactions between the currents flowing in different conductors (proximity effect). This current distribution was used to compute the h.f. p.u.l. resistance matrix of the interconnection. This result is summarized in Section II. The model for the p.u.l. internal impedance matrix is introduced in Section III, where we study its behavior at high and low frequencies. We prove the passivity of the model in Section IV. Passivity entails that the model is causal [2] [3]. It *a posteriori* justifies an otherwise arbitrary model. An application to the simulation of a parallel link is provided in Section V.

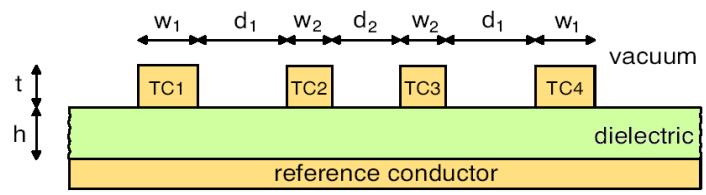

Fig. 1. Cross-section of a multiconductor microstrip interconnection comprising $n = 4$ transmission conductors (TCs) and a reference or ground conductor (GC).

II. High-frequency P.U.L. Resistance Matrix

The MTL model of the interconnection includes the h.f. p.u.l. external inductance matrix of the interconnection, a frequency independent real $n \times n$ matrix denoted by $\mathbf{L}_0$. It may be defined as the per-unit-length inductance matrix computed using the high-frequency current distribution in the conductors.

For simplicity, we assume that the resistivity and the skin depth are the same in all TCs and denoted by ρ_{TC} and δ_{TC}, respectively. At sufficiently high frequencies, the thickness and width of each TC are each much greater than δ_{TC}. The h.f. p.u.l. resistance matrix of the TCs, denoted by $\mathbf{R}_{HFTC}$, is given by [1]

$$\mathbf{R}_{HFTC} = \frac{\rho_{TC}}{\delta_{TC}} \mathbf{K}_{TC} \tag{1}$$

where we refer to $\mathbf{K}_{TC}$ as the matrix of the equivalent inverse widths of the TCs. $\mathbf{K}_{TC}$ can be obtained at a low computational cost using quantities determined during the computation of $\mathbf{L}_0$.

Using ρ_{GC} and δ_{GC} to denote the resistivity and the skin depth of the GC, respectively, the h.f. p.u.l. resistance matrix of the GC, denoted by $\mathbf{R}_{HFGC}$, is given by [1]

$$\mathbf{R}_{HFGC} = \frac{\rho_{GC}}{\delta_{GC}} \mathbf{K}_{GC} \tag{2}$$

where we refer to $\mathbf{K}_{GC}$ as the matrix of the equivalent inverse widths of the GC. $\mathbf{K}_{GC}$ can be obtained at a low computational cost using numerical integrations along the boundary of the GC.

Finally, the h.f. resistance matrix of the interconnection, denoted by $\mathbf{R}_{HF}$, is given by

$$\mathbf{R}_{HF} = \mathbf{R}_{HFTC} + \mathbf{R}_{HFGC} = \frac{\rho_{TC}}{\delta_{TC}} \mathbf{K}_{TC} + \frac{\rho_{GC}}{\delta_{GC}} \mathbf{K}_{GC} \tag{3}$$

The conductors being reciprocal and passive, $\mathbf{K}_{TC}$ and $\mathbf{K}_{GC}$ are frequency-independent real positive semidefinite matrices [4,

§ 7.1]. Thus, any diagonal entry of $\mathbf{K}_{TC}$ or $\mathbf{K}_{GC}$ is non-negative.

As an example, we consider the multiconductor microstrip interconnection shown in Fig. 1, in the case $t = 34.8$ µm, $w_1 = w_2 = d_1 = d_2 = 203.2$ µm and $h = 152.4$ µm. Using the method of moment with pulse expansion and 336 matching points [5, § 3.3], we find that $\mathbf{K}_{TC}$ and $\mathbf{K}_{GC}$ are given by

$$\mathbf{K}_{TC} = \begin{pmatrix} 2814 & 39 & 11 & 14 \\ 39 & 2893 & 58 & 11 \\ 11 & 58 & 2893 & 39 \\ 14 & 11 & 39 & 2814 \end{pmatrix} \mathrm{m}^{-1} \tag{4}$$

and

$$\mathbf{K}_{GC} = \begin{pmatrix} 894 & 427 & 170 & 81 \\ 427 & 872 & 422 & 170 \\ 170 & 422 & 872 & 427 \\ 81 & 170 & 427 & 894 \end{pmatrix} \mathrm{m}^{-1} \tag{5}$$

In (4), all entries of $\mathbf{K}_{TC}$ are nonnegative. However, for other interconnections, we have obtained negative non-diagonal entries in $\mathbf{K}_{TC}$. In all configurations for which we have computed $\mathbf{K}_{TC}$ and $\mathbf{K}_{GC}$, we found that $\mathbf{K}_{TC}$ is strictly diagonally dominant [4, § 6.1.9], and that $\mathbf{K}_{GC}$ is nonnegative [4, § 8.1].

III. A Model for the P.U.L. Internal Impedance Matrix

In this paper, the p.u.l. internal impedance matrix of the interconnection, denoted by $\mathbf{Z}_I$, is given by $\mathbf{Z}_I = \mathbf{Z} - j\omega\, \mathbf{L}_0$, where $\mathbf{Z}$ is the p.u.l. impedance matrix of the interconnection. This definition is not the one used in [6], but it is in line with the one used in [7, § 2.8]. We clearly have $\mathbf{Z}_I = \mathbf{0}$ for lossless conductors.

Complying with Wheeler's incremental-inductance rule [8], we assume that, for frequencies high enough for the skin effect to be well developed, the real and imaginary parts of $\mathbf{Z}_I$ become approximately equal and exhibit a $f^{1/2}$ increase with frequency. Thus, the h.f. p.u.l. internal impedance matrix satisfies

$$\mathbf{Z}_{I\,HF} \approx (1+j)\left(\frac{\rho_{TC}}{\delta_{TC}}\mathbf{K}_{TC} + \frac{\rho_{RC}}{\delta_{RC}}\mathbf{K}_{RC}\right) \tag{6}$$

Wheeler's incremental-inductance rule is not an exact law, but it gives reasonably accurate values for a single conductor [6] [9].

Some authors assume that, in the Laplace domain, $\mathbf{Z}_I$ is given by the model $\mathbf{Z}_S = \mathbf{A} + s^{1/2}\,\mathbf{B}$ where s is the Laplace transform variable and where $\mathbf{A}$ and $\mathbf{B}$ are two frequency independent matrices [5, § 5.3]. $\mathbf{A}$ and $\mathbf{B}$ can be determined such that $\mathbf{Z}_S$ complies with (6) and provides an exact dc resistance matrix. However, $\mathbf{Z}_S$ produces non-physical infinite dc self-inductances and infinite or zero dc mutual inductances. Also, in the case of a single TC of circular cross-section having a coaxial return path, for $s = j\omega$ where ω is real, the model $Z_S = A + B\, s^{1/2}$ produces large errors in the vicinity of the skin-effect onset frequency [7, § 2.8].

In the same case of a single TC of circular cross-section having a coaxial return path, another model assumes that $\mathbf{Z}_I$ is given by $Z_B = (A + B\, s)^{1/2}$. This model is also compatible with (6) and it can provide a good approximation of the exact solution at all frequencies [7, § 2.8]. The accuracy of Z_B in the case of the circular symmetry is caused by the fact that A and B can be chosen such that an exact h.f. impedance, an exact dc resistance and an exact dc inductance are simultaneously obtained. Unfortunately, this miracle does not occur with other single-TC configurations (for instance a TC having a rectangular cross-section) and this model using Z_B does not lend itself to an obvious generalization to $n \geq 2$.

We have tried to define a p.u.l. internal impedance matrix model combining the following properties: being exact at dc; complying with (6); producing finite and reasonable dc self- and mutual inductances; and ensuring passivity. For want of a better approach, we have used a trial-and-failure process in which the most difficult part was the proof of passivity covered in Section IV. This led us to a new model for $\mathbf{Z}_I$, denoted by $\mathbf{Z}_N$ and defined by

$$\mathbf{Z}_N = \mathbf{Z}_{NR} + \mathbf{Z}_{NTC} + \mathbf{Z}_{NGC} \tag{7}$$

where, for the indices α and β ranging from 1 to n with $\alpha \neq \beta$, the entries of the matrices $\mathbf{Z}_{NR}$, $\mathbf{Z}_{NTC}$ and $\mathbf{Z}_{NGC}$ are respectively given by

$$\begin{cases} Z_{NR\alpha\alpha} = R_{DC\alpha} + R_{DCGC} \\ Z_{NR\alpha\beta} = \dfrac{R_{DCGC}}{\sqrt{1 + \dfrac{4sL_{MAXGC}^2}{\mu_0\rho_{GC}\left(\max\limits_{1\leq i\leq n} K_{GCii}\right)^2}}} \end{cases} \tag{8}$$

$$\begin{cases} Z_{NTC\alpha\alpha} = \dfrac{\mu_0\rho_{TC}K_{TC\alpha\alpha}^2}{2L_{MAX\alpha}}\left(\sqrt{1 + \dfrac{4sL_{MAX\alpha}^2}{\mu_0\rho_{TC}K_{TC\alpha\alpha}^2}} - 1\right) \\ Z_{NTC\alpha\beta} = \dfrac{\mu_0\rho_{TC}K_{TC\alpha\beta}\left(\sqrt{1 + \dfrac{4s}{\mu_0\rho_{TC}}\left(\min\left\{\dfrac{L_{MAX\alpha}}{K_{TC\alpha\alpha}}, \dfrac{L_{MAX\beta}}{K_{TC\beta\beta}}\right\}\right)^2} - 1\right)}{2\min\left\{\dfrac{L_{MAX\alpha}}{K_{TC\alpha\alpha}}, \dfrac{L_{MAX\beta}}{K_{TC\beta\beta}}\right\}} \end{cases} \tag{9}$$

and

$$\mathbf{Z}_{NGC} = \frac{\mu_0\rho_{GC}\max\limits_{1\leq i\leq n} K_{GCii}}{2L_{MAXGC}}\left(\sqrt{1 + \frac{4sL_{MAXGC}^2}{\mu_0\rho_{GC}\left(\max\limits_{1\leq i\leq n} K_{GCii}\right)^2}} - 1\right)\mathbf{K}_{GC} \tag{10}$$

where each square root symbol denotes the principal root, where the p.u.l. dc resistances of the TCs are denoted by $R_{DC\,1}$ to $R_{DC\,n}$, the p.u.l. dc resistance of the GC is denoted by R_{DCGC}, the p.u.l. inductances $L_{MAX\,1}$ to $L_{MAX\,n}$ relate to the TCs and the p.u.l. inductance L_{MAXGC} relates to the GC.

Since it comprises several terms in the form $(A + B\, s)^{1/2}$, the model $\mathbf{Z}_N$ can be seen as an extension of the model Z_B, intended to provide a causal and passive approximation for any configuration of the TCs and GC.

The Fig. 2 shows some entries of $\mathbf{Z}_N$ computed with (7)-(10),

for the multiconductor microstrip interconnection considered in Section II. In this computation, L_{MAX1} to $L_{MAX\ n}$ are equal to the p.u.l. dc internal inductance 24.3 nH/m of the identical TCs, computed using a closed-form approximation [10, eq. (30)-(31)]. In this computation, $L_{MAXGC} = L_{DC}/10$. In Fig. 2, we also assume $\rho_{GC} = \rho_{TC} =$ 16.78 nΩ.m and $R_{DCGC} = 4.8$ mΩ/m. We find that the dc internal inductance matrix defined by

$$\mathbf{L}_{I\,DC} = \lim_{\omega \to 0} \frac{\mathrm{Im}\left(\mathbf{Z}_N(j\omega)\right)}{\omega} \tag{11}$$

is given by

$$\mathbf{L}_{I\,DC} = \begin{pmatrix} 26.8 & 1.5 & 0.6 & 0.3 \\ 1.5 & 26.7 & 1.6 & 0.6 \\ 0.6 & 1.6 & 26.7 & 1.5 \\ 0.3 & 0.6 & 1.5 & 26.8 \end{pmatrix} \frac{\mathrm{nH}}{\mathrm{m}} \tag{12}$$

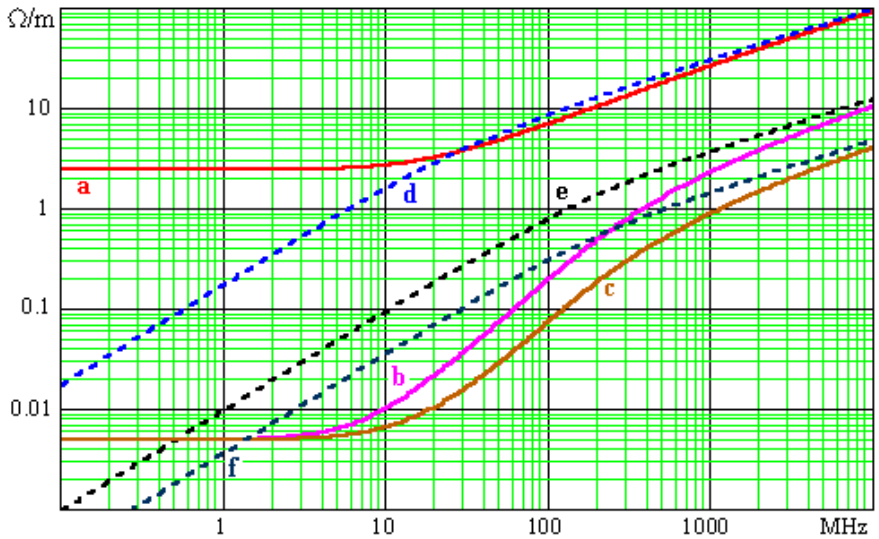

Fig. 2. Some entries of $\mathbf{Z}_N$ versus frequency. Curve a: real part of $Z_{N\,11}$. Curve b: real part of $Z_{N\,12}$. Curve c: real part of $Z_{N\,13}$. Curve d: imaginary part of $Z_{N\,11}$. Curve e: imaginary part of $Z_{N\,12}$. Curve f: imaginary part of $Z_{N\,13}$.

We observe that $\mathbf{Z}_N$ produces finite and reasonable dc self- and mutual inductances. This is in contrast with the model $\mathbf{Z}_S$, in which infinite dc self- and mutual inductances produce various artifacts, which are not easy to detect and sort out in time domain simulations. It can easily be shown that our model has the following characteristics:

- $\mathbf{Z}_N$ is exact at dc;
- $\mathbf{Z}_N$ complies with (6) at frequencies sufficiently high to allow us to neglect the 1 in each square root of (9)-(10) and to neglect $\mathbf{Z}_{NR}$, given by (8), in (7);
- the dc internal inductance produced by $Z_{N\,\alpha\,\alpha}$ ranges between $L_{MAX\ \alpha}$ and $L_{MAX\ \alpha} + L_{MAXGC}$ and, for $\alpha \neq \beta$, the dc internal inductance produced by $Z_{N\,\alpha\,\beta}$ is finite.

IV. Passivity of the Model

We shall outline the proof of the passivity of our model $\mathbf{Z}_N$, based on the following well-known theorem [2, § IV.D] [3].

Theorem on passivity. An impedance matrix $\mathbf{Z}(s)$ represents a passive linear system if and only if

(*i*) each entry of $\mathbf{Z}(s)$ is defined and analytic in the half plane $\sigma > 0$, where $\sigma = \mathrm{Re}(s)$;

(*ii*) $\mathbf{Z}^*(s) + \mathbf{Z}(s)$, where the star indicates the hermitian adjoint, is a positive semidefinite matrix for all s such that $\sigma > 0$;

(*iii*) $\mathbf{Z}(\bar{s}) = \overline{\mathbf{Z}}(s)$, where the bar indicates the complex conjugate.

The conditions (*i*) and (*iii*) are clearly satisfied for the impedance matrices $\mathbf{Z}_N$, $\mathbf{Z}_{NR}$, $\mathbf{Z}_{NTC}$ and $\mathbf{Z}_{NGC}$ defined by (7)-(10). The condition (*ii*) is addressed below.

If r and $m_1, \ldots, m_n$ are real numbers, for any $p \in \{1,\ldots, n\}$ let us use $\mathbf{M}_p(m_1, \ldots, m_p)$ to denote the matrix

$$\mathbf{M}_p\left(m_1,\cdots,m_p\right) = \begin{pmatrix} m_1 & r & \cdots & r \\ r & \ddots & \ddots & \vdots \\ \vdots & \ddots & \ddots & r \\ r & \cdots & r & m_p \end{pmatrix} \tag{13}$$

If for all $\alpha \in \{1,\ldots, n\}$ we have $m_\alpha > r > 0$, we can prove inductively that, for any $p \in \{1,\ldots, n\}$, we have

$$\det\left(\mathbf{M}_p\left(m_1,\cdots,m_p\right)\right) > 0 \tag{14}$$

so that, all elements of a nested chain of n principal minors being positive, $\mathbf{M}_n(m_1, \ldots, m_n)$ is positive definite by [4, § 7.2.5]. A diagonal entry of $\mathbf{Z}_{NR} + \mathbf{Z}_{NR}^*$ is given by

$$Z_{NR\alpha\alpha} + \overline{Z}_{NR\alpha\alpha} = 2\left(R_{DC\alpha} + R_{DCGC}\right) \tag{15}$$

This quantity is positive. A non-diagonal entry of $\mathbf{Z}_{NR} + \mathbf{Z}_{NR}^*$ is given by

$$Z_{NR\alpha\beta} + \overline{Z}_{NR\beta\alpha} = \frac{R_{DCGC}}{\sqrt{1+sE}} + \frac{R_{DCGC}}{\sqrt{1+\bar{s}E}} \tag{16}$$

where $\alpha \neq \beta$ and where E is a positive real number. We see that $\mathbf{Z}_{NR} + \mathbf{Z}_{NR}^*$ is in the form of (13), and it is possible to prove that, if $\sigma > 0$, then for all $\alpha \in \{1,\ldots, n\}$, we have $m_\alpha > r > 0$. Thus, we conclude that the condition (*ii*) is satisfied by $\mathbf{Z}_{NR}$.

$\mathbb{R}_+\backslash\{0\}$ being the set of positive real numbers, let us define a function of $s \in \mathbb{C}$ and $\lambda \in \mathbb{R}_+\backslash\{0\}$, by

$$z(s,\lambda) = \frac{c}{2\lambda}\left(\sqrt{1+\frac{4s\lambda^2}{c}} - 1\right) \tag{17}$$

where $c \in \mathbb{R}_+\backslash\{0\}$. $z(s, \lambda)$ appears 3 times in (9)-(10). It can be shown that:

(*iv*) for $\sigma > 0$, we have $\mathrm{Re}(z(s, \lambda)) > 0$;

(*v*) for $\sigma > 0$, $\mathrm{Re}(z(s, \lambda))$ is an increasing function of λ.

Using (*v*) and the assumption that $\mathbf{K}_{TC}$ is strictly diagonally dominant (see the end of Section II), it is possible to show that if $\sigma > 0$ then $\mathbf{Z}_{NTC} + \mathbf{Z}_{NTC}^*$ is strictly diagonally dominant. Each $K_{TC\,\alpha\,\alpha}$ being positive, by (*iv*) each diagonal entry of $\mathbf{Z}_{NTC} + \mathbf{Z}_{NTC}^*$ is positive for $\sigma > 0$. We conclude that, if $\sigma > 0$ then $\mathbf{Z}_{NTC} + \mathbf{Z}_{NTC}^*$ is positive definite by [4, § 7.2.3]. Thus, the condition (*ii*) is satisfied by $\mathbf{Z}_{NTC}$.

By (*iv*), if $\sigma > 0$, $\mathbf{Z}_{NGC} + \mathbf{Z}_{NGC}^*$ is the product of a positive

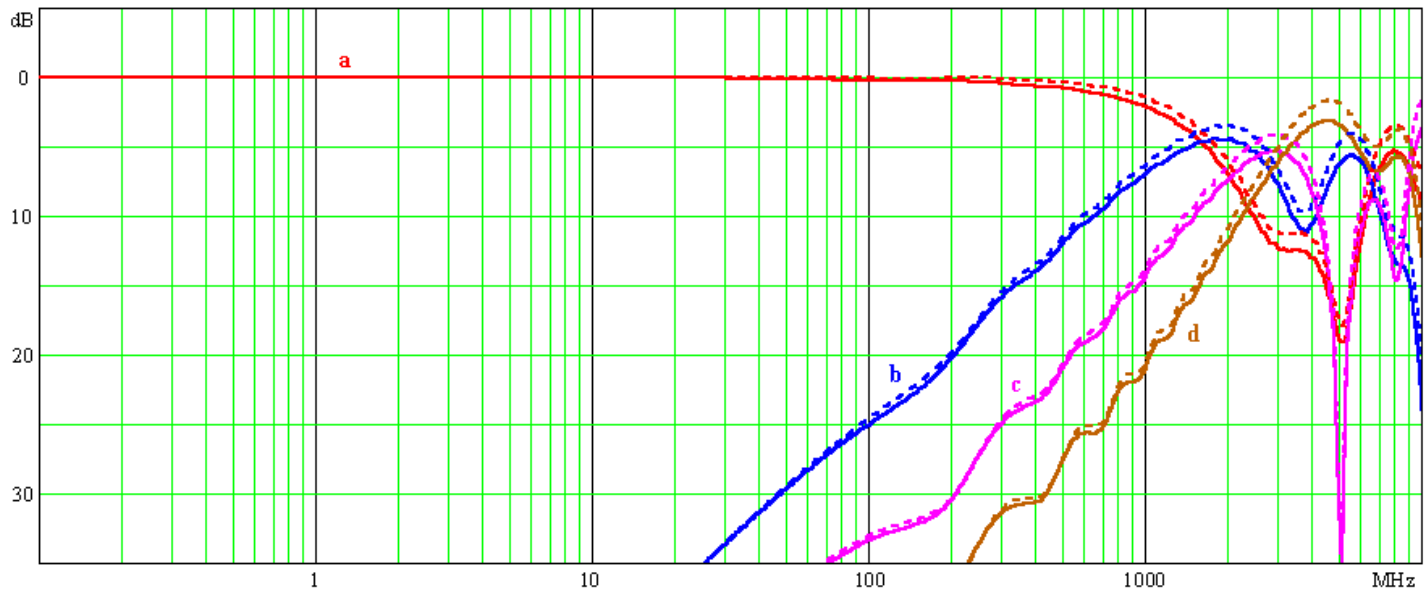

Fig. 3. Attenuation at the far-end when a signal is applied to TC 1, with a lossless model (dashed curves) and our model for resistive losses (solid curves). Curves a: on TC1. Curves b: on TC2. Curves c: on TC3. Curves d: on TC4. Dielectric losses are not taken into account.

constant and the positive definite matrix $\mathbf{K}_{GC}$, so that $\mathbf{Z}_{NGC} + \mathbf{Z}_{NGC}^*$ is positive definite by [4, § 7.1.3] and the condition (*ii*) is satisfied by $\mathbf{Z}_{NGC}$. Moreover, since

$$\mathbf{Z}_N + \mathbf{Z}_N^* = \mathbf{Z}_{NR} + \mathbf{Z}_{NR}^* + \mathbf{Z}_{NTC} + \mathbf{Z}_{NTC}^* + \mathbf{Z}_{NGC} + \mathbf{Z}_{NGC}^* \quad (18)$$

we find that $\mathbf{Z}_N + \mathbf{Z}_N^*$ is positive definite for $\sigma > 0$. Thus, the condition (*ii*) is satisfied by $\mathbf{Z}_N$. We conclude that the impedance matrices $\mathbf{Z}_N$, $\mathbf{Z}_{NR}$, $\mathbf{Z}_{NTC}$ and $\mathbf{Z}_{NGC}$ each represents a passive linear system, and consequently a causal system [2, § III.C] [3].

V. Simulation of a Parallel Link

The model $\mathbf{Z}_N$ can easily be implemented in a frequency domain or time domain simulation tool using a MTL model. For instance, we consider a parallel link comprising the multiconductor microstrip interconnection shown in Fig. 1 and presented in Section II, in the case of a lossless substrate of relative permittivity $\varepsilon_r = 4.65$. We assume a length of 30 cm and that the devices connected at the near-end and at the far-end are seen by the interconnection as linear devices having an impedance matrix equal to 50 Ω × $\mathbf{1}_4$, where $\mathbf{1}_p$ is the identity matrix of size $p \times p$. The Fig. 3 shows the attenuations at the far-end, when a signal is applied to TC 1, computed with our in-house simulation tools.

VI. Conclusion

We have defined a new model for the p.u.l. internal impedance matrix. At high frequencies, it assumes a normal skin effect (i.e., the frequency is not so high that the anomalous skin effect occurs [11, ch. 4]) and it takes into account the edge effect and the proximity effect. This analytical model is physically reasonable and realizable in the sense that it is exact at dc, accurate at high frequencies, corresponds to a finite dc inductance matrix, and that it represents a causal and passive linear system. As far as we know, no other analytical model combines these properties.

Another important attribute of an actual interconnection is that a variable measured at the far-end at a given point in time t is not influenced by any voltage or current at the near-end occurring after t less a suitably defined travel time. This property may be referred to as *transmission-line-causality*. Unlike causality, it is not a direct consequence of passivity. The transmission-line-causality of our model is a subject for further research.

References

[1] F. Broydé, E. Clavelier, "A Simple Computation of the High-Frequency Per-Unit-Length Resistance Matrix", *Proc. of the 15th IEEE Workshop on Signal Propagation on Interconnects, SPI 2011*, May 2011, pp. 121-124.

[2] P. Triverio, S. Grivet-Talocia, M.S. Nakhla, F.G. Canavero and R. Achar, "Stability, causality and passivity in electrical interconnect models", *IEEE Trans. on Advanced Packaging*, vol. 30, No. 7, November 2007, pp. 795-808.

[3] A.H. Zemanian, "An N-port realizability theory based on the theory of distributions", *IEEE Trans. Circuit Theory*, vol. 10, No. 2, pp. 265-274, June 1963.

[4] R.A. Horn, C.R. Johnson, *Matrix analysis*, Cambridge University Press, 1985.

[5] C.R. Paul, *Analysis of Multiconductor Transmission Lines*, John Wiley & Sons, 1994.

[6] A. Rong, A.C. Cangellaris, "Note on the definition and calculation of the per-unit-length internal impedance of a uniform conducting wire", *IEEE Trans. Electromagn. Compat.*, vol. 49, No. 3, August 2007, pp. 677-681.

[7] H. Johnson and M. Graham, *High-Speed Signal Propagation — Advanced Black Magic*, Prentice Hall PTR, 2003.

[8] H.A. Wheeler, "Formulas for the Skin Effect", *Proceedings of the IRE*, vol. 30, No. 9, Sept. 1942, pp. 412-424.

[9] G. Antonini, A. Orlandi and C.R. Paul, "Internal Impedance of Conductors of Rectangular Cross Section", *IEEE Trans. on Microwave Theory Tech.*, vol. 47, No. 7, July 1999, pp. 979-985.

[10] C.L. Holloway and E.F. Kuester, "DC Internal Inductance for a Conductor of Rectangular Cross Section", *IEEE Trans. Electromagnetic Compatibility*, vol. 51, No. 2, May 2009, pp. 338-344.

[11] R.E. Matick, *Transmission lines for digital and communication networks*, McGraw-Hill, 1969.